Published OnlineFirst April 3, 2018; DOI: 10.1158/0008-5472.CAN-17-3140

Translational Science

Cancer Research

Adoptive Immunotherapy Using PRAME-Specific T Cells in Medulloblastoma

Domenico Orlando[1], Evelina Miele[1], Biagio De Angelis[1], Marika Guercio[1], Iolanda Boffa[1], Matilde Sinibaldi[1], Agnese Po[2], Ignazio Caruana[1], Luana Abballe[3], Andrea Carai[4], Simona Caruso[1], Antonio Camera[1], Annemarie Moseley[5], Renate S. Hagedoorn[6], Mirjam H.M. Heemskerk[6], Felice Giangaspero[7,8], Angela Mastronuzzi[1], Elisabetta Ferretti[3,8], Franco Locatelli[1,9], and Concetta Quintarelli[1,10]

Abstract

Medulloblastoma is the most frequent malignant childhood brain tumor with a high morbidity. Identification of new therapeutic targets would be instrumental in improving patient outcomes. We evaluated the expression of the tumor-associated antigen PRAME in biopsies from 60 patients with medulloblastoma. PRAME expression was detectable in 82% of tissues independent of molecular and histopathologic subgroups. High PRAME expression also correlated with worse overall survival. We next investigated the relevance of PRAME as a target for immunotherapy. Medulloblastoma cells were targeted using genetically modified T cells with a PRAME-specific TCR (SLL TCR T cells). SLL TCR T cells efficiently killed medulloblastoma HLA-A*02$^+$ DAOY cells as well as primary HLA-A*02$^+$ medulloblastoma cells. Moreover, SLL TCR T cells controlled tumor growth in an orthotopic mouse model of medulloblastoma. To prevent unexpected T-cell–related toxicity, an inducible caspase-9 (iC9) gene was introduced in frame with the SLL TCR; this safety switch triggered prompt elimination of genetically modified T cells. Altogether, these data indicate that T cells genetically modified with a high-affinity, PRAME-specific TCR and iC9 may represent a promising innovative approach for treating patients with HLA-A*02$^+$ medulloblastoma.

Significance: These findings identify PRAME as a medulloblastoma tumor-associated antigen that can be targeted using genetically modified T cells. *Cancer Res; 78(12); 3337–49. ©2018 AACR.*

Introduction

Medulloblastoma (MB) is the most frequent malignant brain tumor in childhood. Multimodal treatment, including surgical resection, chemotherapy, and radiation, results in good cure rates (1). However, about 30% of children still die because of the disease, recurrences being virtually incurable (2, 3). Moreover, long-term survivors frequently face undesirable effects of treatment, which can significantly impair their quality of life. Improvement of cure rate and of long-term quality of life in this population is a priority currently addressed by ongoing clinical trials.

We chose to explore the feasibility of adoptive immunotherapy using PRAME (an antigen preferentially expressed in melanoma) as a target for treatment of patients with medulloblastoma. PRAME was originally identified as a gene coding for HLA-A*24–presented antigens, able to stimulate tumor-specific cytotoxic lymphocytes (CTL) derived from patients with melanoma (4). PRAME belongs to the cancer-testis antigens (CTA) family, and its expression has been demonstrated in several tumors (including melanoma, non–small cell lung carcinoma, breast carcinoma, renal cell carcinoma, head and neck cancer, Wilms' tumor and Hodgkin lymphoma) and in germline tissues, whereas it has limited expression in healthy adult tissues (5). These features make PRAME a suitable target antigen for tumor immunotherapy (6, 7). Despite the possibility of *in vitro* reactivation of progenitor T cells specifically directed against PRAME peptides able to target leukemia HLA-matched cells (8–10), this approach remains difficult to translate into clinical application, for several reasons, including availability of GMP-grade reagents, the need to generate autologous antigen-presenting cells, as well as the prolonged *in vitro* culture needed to generate clinically meaningful numbers of specific T cells.

We preliminary chose to evaluate PRAME expression in biopsies of medulloblastoma, collected either at diagnosis or at relapse, to investigate the feasibility of targeting medulloblastoma cells by adoptive cell therapy using polyclonal T cells genetically modified through PRAME-specific high-affinity αβTCR. In particular, in our approach, we used the previously identified high-affinity allo-HLA–restricted TCR, specific for the PRAME-SLL

[1]Department of Pediatric Haematology and Oncology, IRCCS Ospedale Pediatrico Bambino Gesù, Rome, Italy. [2]Department of Molecular Medicine, Sapienza University of Rome, Rome Italy. [3]Department of Experimental Medicine, Sapienza University of Rome, Rome, Italy. [4]Department of Neuroscience and Neurorehabilitation, Neurosurgery Unit, IRCCS Ospedale Pediatrico Bambino Gesù, Roma, Italia. [5]Bellicum Pharmaceuticals, Inc. Houston, Texas. [6]Department of Hematology, Leiden University Medical Center, Leiden, the Netherlands. [7]Department of Radiological, Oncological and Pathological Science, Sapienza University of Rome, Rome, Italy. [8]Neuromed Institute, Pozzilli, Italy. [9]Department of Paediatric Sciences, University of Pavia, Pavia, Italy. [10]Department of Clinical Medicine and Surgery, University of Naples Federico II, Naples, Italy.

Note: Supplementary data for this article are available at Cancer Research Online (http://cancerres.aacrjournals.org/).

D. Orlando, E. Miele, and B. De Angelis are the co-first authors of this article.

F. Locatelli and C. Quintarelli are the co-last authors of this article.

Corresponding Author: Biagio De Angelis, IRCCS Ospedale Pediatrico Bambino Gesù, Viale di San Paolo, 15, Roma 00146, Italy. Phone: 3906-6859-4348; E-mail: biagio.deangelis@opbg.net

doi: 10.1158/0008-5472.CAN-17-3140

Published OnlineFirst April 3, 2018; DOI: 10.1158/0008-5472.CAN-17-3140

peptide (SLL TCR), which exerts single-peptide, highly specific activity against a large number of malignancies and limited on-target off-tumor toxicity (11, 12). We also included in the construct a new suicide gene, known as inducible caspase-9 (iC9; ref. 13) in frame with SLL TCR to guarantee prompt elimination of the genetically modified cells in case of undue life-threatening toxicity. In particular, the induction of iC9 depends on the administration of the small molecule, dimerizing drug AP1903 and dimerization results into rapid induction of apoptosis in transduced cells. The *iC9* gene has been incorporated into vectors for use in preclinical studies and was shown to be an effective and reliable suicide gene activity in phase I clinical trials (14).

Materials and Methods

Cell lines

The following cell lines: DAOY (desmoplastic cerebellar medulloblastoma, HLA-A*02+), D283 Med (medulloblastoma, down-regulated HLA-A*02), CEMT2 (hybrids of human T and B lymphoblastoid cell lines, HLA-A*02+), RS4:11 (acute lymphoblastic leukemia, HLA-A*02-), U266 (myeloma, HLA-A*02+), HDML2 (Hodgkin lymphoma, HLA-A*02-), and HEK 293T/17 (embryonic human kidney used to produce retroviral supernatant), were obtained from the ATCC. RS4:11, U266, HDML2, and CEM-T2 were maintained in culture with RPMI1640 medium (EuroClone). DAOY and D283 MB cells were cultured in Iscove's modified Dulbecco's medium (EuroClone), while HEK 293T/17 in DMEM (EuroClone). Mediums contain 10% heat-inactivated, FBS (EuroClone), 2 mmol/L L-glutamine (GIBCO), 25 IU/mL of penicillin, and 25 mg/mL of streptomycin (EuroClone). Cells were maintained in humidified atmosphere containing 5% CO_2 at 37°C. Identity of all cell lines was confirmed by an external lab (BMR Genomics srl) through PCR-single-locus-technology (Promega, PowerPlex 21 PCR); mycoplasma test was performed every three months.

Healthy donors' PBMCs, patients with medulloblastoma, and controls

Peripheral blood mononuclear cells (PBMC) were isolated from either peripheral blood or buffy coat obtained from 8 healthy donors after obtaining written informed consent, in accordance with rules set by the Institutional Review Board of Bambino Gesù Children's Hospital of Rome (OPBG, Approval of Ethical Committee No. 969/2015 prot. No. 669LB), using Lymphocyte Separation Medium (Eurobio). Medulloblastoma specimens were obtained from a cohort of 60 patients with histologically confirmed diagnosis who had undergone surgical resection at the OPBG between August 2011 and April 2015. All specimens were formalin-fixed, sectioned, stained with hematoxylin and eosin (H&E) and examined through microscopy. To minimize inter-observer variability, histology was reviewed by an experienced neuropathologist, F. Giangaspero, according to the international staging system for pediatric brain tumors (15, 16). The investigation was approved by the Institutional Review Board (Prot. N. 21LB; Study N 730/2013 OPBG). Informed consent was obtained from patient's parents or legal guardians (as required per institutional review board policy). For all samples, around 0.5 cm^3 of tumor tissue was also snap-frozen in liquid nitrogen and stored at −80°C until ready for RNA extraction. Clinical (age, gender and outcome), molecular and histopathologic details of all 60 patients, and of the 51 of them followed in our Institution are reported in Table 1. RNA of normal human cerebellum (10 adult samples from 25- to 70-year-old subjects and 8 samples from 22- to 36-week-old fetuses) was purchased from Biocat, Ambion, and BD Biosciences. Medulloblastoma primary cell lines were obtained from fresh patient's tissue samples. In detail, tissues were collected in HBSS media (Thermo Fisher Scientific) supplemented with 0.5% glucose and 2% penicillin/streptomycin, grossly triturated with serologic pipette and treated with DNAse-I (Sigma-Aldrich) to a final concentration of 0.04% for 20 minutes. Finally, cell aggregates were mechanically dissociated using pipettes of decreasing bore size to obtain a single-cell suspension that was grown in DMEM/F12 medium + 10% FCS and 2% penicillin/streptomycin at 5% CO_2. After 1 week, the supernatant was removed from cultures and replaced with fresh medium. Two weeks after the start of the culture, cells were harvested and characterized for the expression of PRAME and neural markers (B3TUBB, S100A, GFAP) and replated to perform the experiments. In selected experiments, cell lines or primary medulloblastoma patient–derived cells were pretreated with 1,000 IU/mL of IFNγ (R&D Systems) for 48 hours before their use as target cells.

Retroviral constructs

The complete PRAME-specific αβTCR recognizing SLL peptide in the context of HLA-A*02 (11) was cloned in a retroviral vector containing in frame the iC9 suicide gene sequence (iC9-SLL TCR). An additional retroviral vector encoding eGFP-Firefly-Luciferase (eGFP-FFLuc; ref. 17) was used in selected experiments to label tumor cells (DAOY-FF-Luc.GFP and RS4:11-FF-Luc.GFP) for *in vitro* and *in vivo* studies, as described previously (18).

Generation and expansion of polyclonal iC9-SLL TCR T cells

T lymphocytes were activated with immobilized OKT3 (1 μg/mL, eBioscience Inc.) and anti-CD28 (1 μg/mL, BD Biosciences) antibodies in the presence of recombinant human IL2 (100 U/mL; R&D Systems). Activated T cells were transduced on day 3 in 24-well plates precoated with recombinant human RetroNectin (Takara-Bio), using a SFG retroviral supernatant specific for iC9-SLL TCR. On day 5 from transduction, T cells were expanded in "complete medium" containing 45% RPMI1640 and 45% Click medium (Sigma-Aldrich) supplemented with 10% FBS and 2 mmol/L Glutamax, and fed twice a week with IL2 (50 U/mL). In selected experiments, iC9-SLL TCR T cells were generated from $CD8^+$ or $CD4^+$ T cells prepared by positive immunomagnetic sorting (Miltenyi Biotec), following the manufacturer's instructions. iC9-SLL TCR T cells were also sorted by anti-allophycocyanin (APC) magnetic microbeads (Miltenyi Biotec), to select T cells previously stained with SLL-dextramers conjugated with APC (JPT).

Activation of the suicide gene

The chemical inducer of dimerization (CID; AP1903; ARIAD Pharmaceuticals) was kindly provided by Bellicum Pharmaceuticals and added at the indicated concentrations to either control T cells or iC9-SLL TCR T cells. The elimination of transgenic cells coexpressing the *iC9* suicide gene was evaluated 24 to 48 hours later by FACS analysis, enumerating the percentage of $AnnexinV^-/7\text{-}AAD^-$ $V\beta1^+$ $CD3^+$ T cells in the culture.

Immunophenotyping

Expression of cell surface molecules was evaluated by flow cytometry using standard methodology. The following mAbs were used: SLL dextramer conjugated with APC (JPT); CD3

Published OnlineFirst April 3, 2018; DOI: 10.1158/0008-5472.CAN-17-3140

peridinin chlorophyll protein (PerCP)-conjugated mAb; CD8 fluorescein isothiocynate (FITC)-conjugated mAb; T-cell receptor-Vβ1 phycoerythrin (PE)-conjugated mAb (all antibodies were purchased from Becton Dickinson). Control samples, labeled with an appropriate isotype-matched antibody, were included in each experiment. Samples were analyzed with a BD LSRFortessa X-20. Flow cytometry profiles were analyzed using the FACSDiva software (BD Biosciences). For each sample, we analyzed a minimum of 100,000 events.

ELISpot assay

We used an IFNγ ELISpot assay, as described previously (10). Briefly, iC9-SLL TCR T cells were plated in triplicate, serially diluted from 1×10^5–1×10^4 cells/well, and then CEM-T2 (at the ratio 1:1) loaded with either the specific SLL peptides or ALY-PRAME–derived irrelevant peptide were added at the indicated concentration (all peptides from JPT were dissolved in DMSO as indicated by the manufacturer). As a positive control, T cells were stimulated with 25 ng/mL of phorbol myristate acetate (PMA) and 1 μg/mL of ionomycin (Sigma-Aldrich). The $IFN\gamma^+$ spot-forming cells (SFC) were enumerated (ZellNet).

Coculture assays

For coculture experiments, untransduced control (CNT) and iC9-SLL TCR T cells were plated at 0.5×10^6 cells/well in 24-well plates at the indicated effector:target (E:T) ratios (1:1 and 5:1). Following 7 days of incubation at 37°C, adherent tumor cells and T cells were collected, and both residual tumor cells and T cells assessed by FACS analysis based on CD3 expression (effector T cells) and GFP [(DAOY-FF-Luc.GFP cell line (PRAME+HLA-A*02+) and RS4:11-FF-Luc.GFP cell line (PRAME+ HLA-A*02neg.ve)].

IFNγ ELISA

Supernatant from E:T coculture was collected at 24 hours to measure IFNy released by iC9-SLL TCR T or NT T cells. The supernatant was analyzed by ELISA assay (R&D Systems), following the manufacturer's instructions.

Chromium-release assay

The cytotoxic specificity of T cells was evaluated using a standard 4-hour ^{51}Cr-release assay. Target cells were incubated in medium alone or in 1% Triton X-100 (Sigma-Aldrich) to determine spontaneous and maximum ^{51}Cr release, respectively. iC9-SLL TCR T cells or NT T cells were plated in triplicate on $PRAME^+$ $HLA\text{-}A^*02^+$ target cells [DAOY, CEM-T2 or CEM-T2 SLL (loaded with SLL-PRAME peptide) cell line] or on $PRAME^+$ $HLA\text{-}A^*02^-$ target cells (RS4:11 and D283). In selected experiments, we used sorted $CD8^+$ T cells transduced with iC9-SLL TCR as effector cells. After 6 hours of coculture of effector and target cells, as described previously (8), the supernatant was collected and radioactivity measured with a gamma counter. The mean percentage of specific lysis of triplicate wells was calculated as follows: [(experimental release−spontaneous release)/(maximal release-spontaneous release)] × 100.

RNA isolation and quantitative real-time PCR

Total RNA was purified and reverse transcribed (Thermo Scientific) as described previously (19, 20). Quantitative RT-PCR (qRT-PCR) was performed employing Viia7 Sequence Detection System (Thermo Scientific), using best coverage TaqMan gene expression assays, specific for each mRNA analyzed (PRAME, bIII-tubulin S100A, GFAP, GAPDH, β-ACTIN, and β2-MICROGLOBULIN). Expression signature for medulloblastoma subgrouping was performed by qRT-PCR using TaqMan probes, as reported previously (21). TaqMan Low Density Array was custom-designed with TaqMan assays for genes of interest (22). Each amplification was performed in triplicate, and the average of the three threshold cycles was used to calculate the amount of transcripts (Thermo Scientific). Transcript quantification was expressed in arbitrary units (AU) as the ratio of the sample quantity to the mean values of control samples (PBMCs of 8 healthy donors). Relative gene expression was calculated using the $2(2\Delta C_t)$ method, where DCt indicates the differences in the mean cycle threshold (C_t; ref. 23) between selected genes and three endogenous gene controls (GAPDH, β-ACTIN, and β2-MICROGLOBULIN; data were shown only with respect to β-ACTIN normalization.

Molecular detection of retroviral-transduced T cells

Total DNA was purified according to manufacturer indications (Qiagen). Retroviral vector was amplified by using TaqMan probe/primers directed towards an invariant region of the plasmid located between LTR and the transgene iC9-SLL TCR. Vector copy numbers for cells were normalized with respect to the copy numbers of the housekeeping gene β-Actin.

Xenograft mouse model for *in vivo* studies

All immunocompromised NSG (NOD scid gamma) mice (strain NOD.Cg-Prkdc^{scid} Il2rg^{tm1Wjl}/SzJ) were purchased from Charles River and maintained in the animal facility at Sapienza University (where orthotopic models using stereotaxic medulloblastoma implantation in mouse brains were performed) or in *Plaisant Castel Romano* (where intraperitoneal model for the bioluminescence monitoring of the tumor using IVIS Image System was performed) in Rome. All procedures were performed in accordance with the Guidelines for Animal Care and Use of the NIH (Ethical committee for animal experimentation Prot. N 03/2013 for University of Rome Sapienza, and Prot. N 088/2016-PR for *Plaisant Castel Romano*, respectively). For the orthotopic *in vivo* model, adult female NSG mice were anesthetized by intraperitoneal injection of ketamine (10 mg/kg) and xylazine (100 mg/kg). The posterior cranial region was shaved and placed in a stereotaxic head frame. DAOY cells were prepared from fresh culture to ensure optimal viability. Medulloblastoma cells (2×10^5 per 5 μL) were stereotaxically implanted into the cerebellum at an infusion rate of 1 μL/minute by using the following coordinates, according to the atlas of Franklin and Paxinos: 6.6 mm posterior to the bregma; 1 mm lateral to the midline; and 2 mm ventral from the surface of the skull. After injection, the cannula was kept in place for about 5 minutes for equilibration of pressures within the cranial vault. The skin was closed over the cranioplastic assembly using metallic clips. Ten days following tumor implantation, the animals were randomly divided into three groups: group 1 = intracranial injection of CTRL -T lymphocytes (10^7); group 2: intracranial injection of PRAME-T lymphocytes (10^7); group 3: no lymphocyte injection. In selected experiments, T cells were inoculated intravenously into the tail vein. On the same day of T-cell infusion, IL2 intraperitoneal treatment was started (1,000 U/animal in PBS; administered twice a week). After 4 weeks, animals were sacrificed and brains were fixed in 4% formaldehyde in 0.1 mol/L phosphate buffer (pH 7.2)

Published OnlineFirst April 3, 2018; DOI: 10.1158/0008-5472.CAN-17-3140

and paraffin embedded. For brain tumor volume calculation, serial thick coronal sections (2 μm) starting from the mesencephalon to the end (HALF) of cerebellum were performed. To *in vivo* estimate tumor control within a setting of bulky tumor, we also carried out an intraperitoneal model of medulloblastoma. In particular, in NSG male mice of 5 weeks age, we engrafted 2×10^6 PRAME$^+$ tumor cells i.p. (DAOY-FF-Luc.GFP) resuspended in Matrigel (Becton Dickinson). Ten days later, when the light emission of the tumor was consistently measurable, mice received intraperitoneal injection of 10^7 iC9-SLL TCR T cells or control, untransduced T cells. Tumor growth was evaluated using IVIS imaging system (PerkinElmer). Briefly, a constant region of interest was drawn over the tumor regions and the intensity of the signal measured as total photon/sec/cm^2/sr (p/s/cm^2/sr), as described previously (24).

Histologic and IHC data

The histopathologic H&E analysis for the orthotopic models was performed on 40 sections (2 μm each), sampled every 40 μm on the horizontal plan of the cerebellum, in which the cerebellum was identified and outlined at ×2.5 magnification. Tumor area of every slice was evaluated with a microscope (Axio Imager M1 microscope; Leica Microsystems GmbH) equipped with motorized stage and Image Pro Plus 6.2 software. The following formula was used to calculate the mouse brain tumor volume: tumor volume = sum of measured area for each slice × slice thickness × sampling frequency.

For IHC analysis, the sections were deparaffinized with xylene, sequentially rehydrated in ethanol, and incubated in 0.3% hydrogen peroxide for 10 minutes to quench endogenous peroxidase activity. Immunostaining was performed using the Vectastain Elite ABC kit (Vector Laboratories). Nonspecific binding was blocked by incubation with normal rat serum for 30 minutes. The sections were then incubated with anti-CD3 antibody (1:100, DAKO) or anti-PRAME (1:100, Abcam) at 4°C for 60 minutes. Sections were incubated with a biotinylated secondary antibody (anti-mouse or anti-rabbit IgG) for 30 minutes, washed, and incubated for another 30 minutes with ABC (avidin and biotinylated enzyme complex) reagent. Color was developed by adding peroxidase substrate diaminobenzidine. Sections were counterstained with Mayer hematoxylin (Sigma-Aldrich) and, finally, mounting solution and coverslips were added.

Mouse behavioral studies

Mice were stereotaxically implanted with DAOY (0.2×10^6/mouse). Ten days after, CNT or iC9-SLL TCR T cells (1×10^7 cells/mouse) were inoculated intravenously into the tail vein. To evaluate the neurologic effect of potential side effects due to T-cell expansion, beginning on day before T cell infusion, throughout the period of tumor eradication (day 14), all the animals ($n = 8$; 4 in each cohort of treatment) were assessed using a modified Smith-Kline Beecham, Harwell, Imperial College, Royal London Hospital, phenotype assessment (SHIRPA) protocol (25). This comprehensive behavioral assessment involves a battery of 33 semiquantitative tests for general health and sensory function, baseline behaviors, and neurologic reflexes. The procedures were carried out in an open testing environment away from the home cage, and took 15–20 minutes per animal daily.

Statistical analysis

All data are presented as means ± SD. Student *t* test was used to determine the statistical differences between samples, and $P < 0.05$ was considered to be statistically significant. Maximum likelihood method (26) using R2: Genomics Analysis and Visualization Platform (http://r2.amc.nl) was applied to calculate the expression level of 19.2×10^3 AU as cutoff to stratify patients based on PRAME expression. The Kaplan–Meier method was used to estimate overall survival (OS) probabilities; differences between groups were compared with the log-rank test. HR for death was calculated with 95% confidence interval (CI). No evaluable samples were excluded from the analyses. Animals were excluded only in the event of death after tumor implant, but before T-cell infusion. Neither randomization nor blinding was done during the *in vivo* study. However, mice were matched on the basis of the tumor signal for control and treatment groups before infusion of control or gene-modified T cells in the intraperitoneal bulky medulloblastoma tumor model. In this last model, to evaluate tumor growth over time, bioluminescence signal intensity was collected in a blind fashion. Bioluminescence signal intensity was log transformed and then compared using a two-sample *t* test. The analysis of the neuropathologist (F. Giangaspero), aimed at quantifying tumor volume, was performed in a blind fashion. We estimated the sample size considering the variation and average of the samples. We tried to reach a conclusion using a sample size as small as possible. We estimated the sample size to detect a difference in averages of 2 SD at the 0.05 level of significance with an 80% power. Graph generation and statistical analyses were performed using Prism version 6.0d software (GraphPad).

Results

PRAME expression in medulloblastoma at diagnosis and relapse

Bioinformatics analysis of gene expression datasets reveals that the majority of known CTAs are either downregulated (Supplementary Fig. S1) or not modulated (Supplementary Fig. S2) in medulloblastoma samples with respect to normal cerebellum, the only exception being represented by PRAME (Supplementary Fig. S3A and S3B) and CT22 (a CT-antigen, also known as Sperm Autoantigenic Protein 17 - SPA17, with a wide expression in somatic tissues; ref. 27).

In light of these findings, we decided to focus our study on PRAME, investigating its mRNA expression levels in 10 normal adult (NAHC) and 8 fetal cerebella (NFHC), observing negligible expression with respect to mononuclear cells derived from 8 healthy donors (PBMC; Fig. 1A).

We then evaluated PRAME mRNA levels in tumor samples collected at diagnosis from 60 patients with medulloblastoma diagnosed/treated at OPBG. The clinicopathologic data of the considered patients with medulloblastoma are summarized in Table 1. In 82% (49/60) of all tumor samples, we observed a PRAME expression higher (average, $92.2 \times 10^3 \pm 248 \times 10^3$; range, 0.9×10^3-$1{,}500 \times 10^3$ AU) than that of NAHC tissues (average, 0.8×10^3 AU; $P < 0.0001$), with no relevant differences among the four molecular subgroups (Fig. 1A).

Importantly, Kaplan–Meier analysis showed that high PRAME mRNA expression correlates significantly with a worse OS probability in the 51 patients for which follow-up data were available

Published OnlineFirst April 3, 2018; DOI: 10.1158/0008-5472.CAN-17-3140

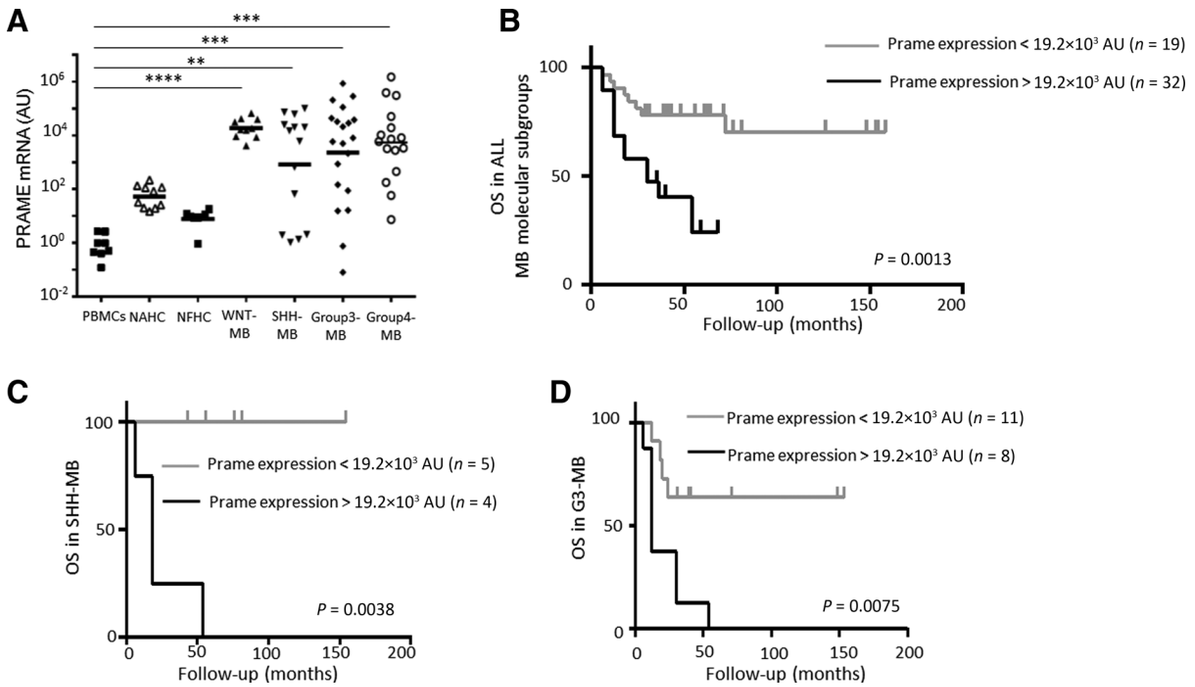

Figure 1.

PRAME mRNA expression and its correlation with clinical feature of medulloblastoma (MB). **A,** Relative expression of PRAME mRNA in PBMCs isolated from 8 healthy donors, 10 normal adult human cerebella (NAHC), 8 normal fetal human cerebella (NFHC), biopsies from 10 patients with medulloblastoma WNT pathway subtype (WNT-MB), 14 patients with medulloblastoma SHH pathway subtype (SHH-MB), 20 patients with Group 3-MB, and 16 patients with Group 4-MB. Transcripts quantification was expressed in AU versus the average expression of PRAME mRNA observed in PBMCs isolated from 8 healthy donors. * $P \leq 0.05$; ** $P \leq 0.001$; *** $P \leq 0.0001$; ****, $P \leq 0.00001$. **B,** Kaplan–Meier analysis for OS in all 51 patients with medulloblastoma with a known follow-up ($n = 51$), stratified by PRAME mRNA expression >19.2 $\times$ 10^3 AU or $\leq$ 19.2 $\times$ 10^3 AU, respectively. Differences between groups were compared with the log-rank test. **C** and **D,** Kaplan–Meier analysis for OS in patients with SHH-MB (**C**) and G3-MB (**D**) with more than 5 years of follow-up ($n = 51$), stratified by PRAME mRNA expression >19.2 $\times$ 10^3 AU or $\leq$ 19.2 $\times$ 10^3 AU, respectively.

Table 1. Summary of the clinical, pathologic, and molecular features of patients with medulloblastoma investigated for PRAME expression

		PRAME Expression			PRAME Expression			
Variable	**No. of Dx *n* = 60**	**HIGH[a] *n* = 23**	**LOW[b] *n* = 37**	***P* X^2 test**	**No. of MB pts with known FU *n* = 51**	**HIGH[a] *n* = 19**	**LOW[b] *n* = 32**	***P*** χ^2 **test**
Age				0.4199				0.2108
Infant ($\leq$ 3 years)	12	4	8		9	5	4	
Children (> 3 years $\leq$ 17 years)	47	18	29		42	14	28	
Adults (>17 years)	1	1	0		0	0	0	
Gender				0.0279				0.0459
Male	39	11	28		33	9	24	
Female	21	12	9		18	10	8	
Molecular subgroup				0.6342				0.5307
WNT	10	4	6		9	4	5	
SHH	14	6	8		9	4	5	
Group 3	20	9	11		19	8	11	
Group 4	16	4	12		14	3	11	
Histology				0.1422				0.1188
Desmoplastic	11	4	7		9	2	7	
Classic	36	11	25		30	10	20	
Anaplastic/large cell	13	8	5		12	7	5	
Tumor material				0.0681				0.0612
Primary	58	21	37		49	17	32	
Recurrence	2	2	0		2	2	0	
Status				0.001				0.001
Dead	20	13	7		20	13	7	
Alive	31	6	25		31	6	25	
Alive with <5 year FU	9	4	5					

Abbreviation: FU, follow-up.

[a]High PRAME expression > 19.2 $\times$ 10^3 AU.

[b]Low PRAME expression < 19.2 $\times$ 10^3 AU.

Published OnlineFirst April 3, 2018; DOI: 10.1158/0008-5472.CAN-17-3140

in our Institution. This correlation remains statistically significant considering the PRAME mRNA expression cutoff as the maximum likelihood estimation threshold (24) of 19.2×10^3 AU ($P = 0.0004$; Fig. 1B), the median value of 7.705×10^3 AU ($P = 0.0003$; Supplementary Fig. S4A), the first quartile value of 0.381×10^3 AU ($P = 0.002$; Supplementary Fig. S4B), and third quartile value of 36.221×10^3 AU ($P = 0.0006$; Supplementary Fig. S4C) quartile. Indeed, the median overall survival was 29.1 months (95% CI, 6–62) in high-PRAME-expressing patients group versus 59.4 months (95% CI, 6–158) in low-PRAME-expressing patients group ($P = 0.0004$; Fig. 1B. HR for death, 4.258; 95% CI, 2.288–15.39; $P = 0.0031$). When we stratified patients according to the molecular subgroup, we confirmed a significant correlation between high PRAME expression and worse OS in SHH-MB ($n = 9$; Fig. 1C, $P = 0.0038$) and G3-MB ($n = 19$; Fig. 1D, $P = 0.0075$) subgroups; this correlation was not statistically significant in WNT-MB ($n = 9$) and G4-MB ($n = 14$) possibly because of the low number of patients available. PRAME expression also correlated in our patient's cohort with male gender ($P = 0.0279$).

In two patients with medulloblastoma (one case of SHH-MB and one of Group 3-MB) for which tumor biopsies were available both at diagnosis and at time of relapse, we also investigated PRAME expression, showing that recurrent medulloblastomas expressed high level of the antigen (Supplementary Fig. S5).

Moreover, IHC analysis shows that PRAME protein is also highly expressed in medulloblastoma tumor specimens, ranging from 20% to more than 90% of positivity in tumor cells, whereas the expression of PRAME protein is negligible in normal brain (Supplementary Fig. S6).

Retroviral vector carrying iC9 and PRAME-SLL–specific αβTCR allows stable and functional expression of the transgenes

α and β chains of a TCR specific for PRAME-SLL (11) were cloned, codon-optimized, and encoded into a retroviral vector in frame with iC9 sequences (iC9-SLL TCR; Fig. 2A). Either primary T cells or $CD8^+$ sorted T cells from healthy donors were transduced with the generated retrovirus and expanded in the presence of IL2. Six days after transduction, 53%±8.6% of $CD3^+$ T cells stained for TCRVβ1 (to which PRAME-SLL TCR β chain belongs) and 32%±7.8% of $CD8^+$ T cells with the SLL dextramer (Fig. 2B shows an explicative example, whereas the median level of transduction reached in 8 independent experiments is shown in Fig. 2C). Also $CD4^+$ T cells were significantly transduced with iC9-SLL TCR, as shown by the expression of TCRVβ1; however, the detection of SLL-TCR pairing in $CD4^+$ cells was not possible, as SLL-dextramer staining is specific only

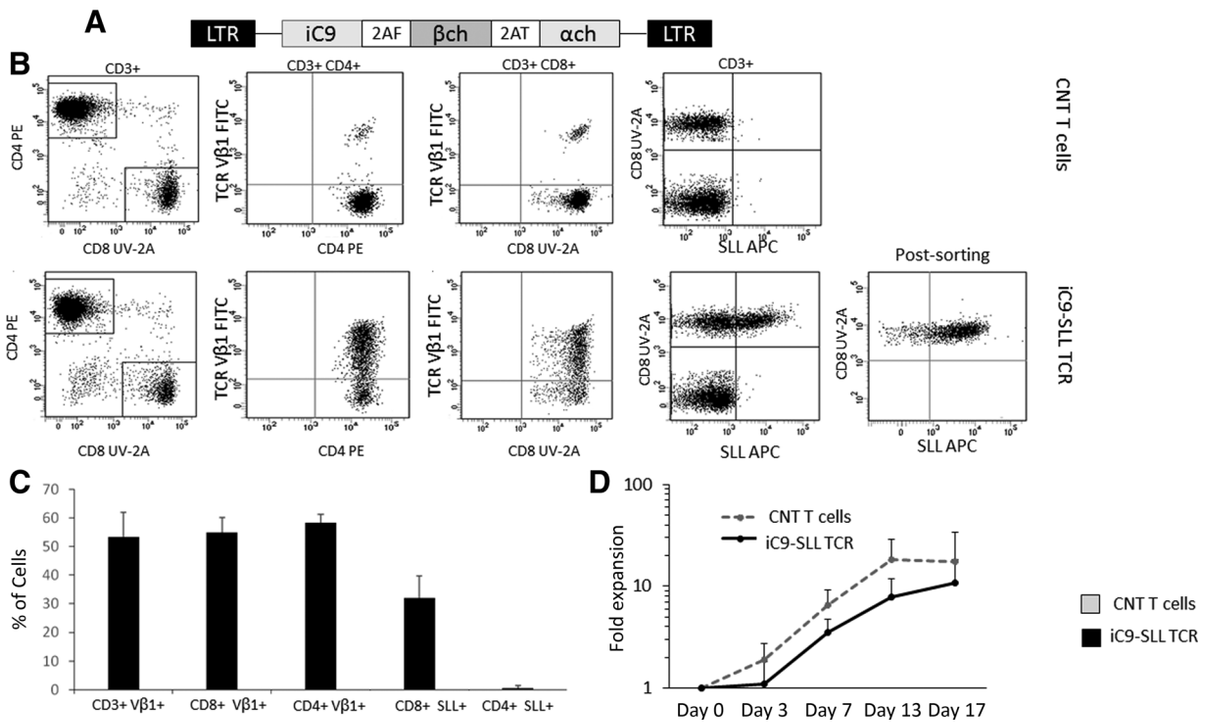

Figure 2.

Generation of iC9-SLL TCR T cells. **A,** α and β chains of SLL-PRAME TCR were cloned in frame with the suicide gene iC9 in a retroviral vector, with the separation of the transgenes through 2A sequences. **B,** Flow cytometry analyses in an esemplificative donor of untransduced (CNT T cells, top) or transduced with the retroviral vector iC9-SLL TCR (bottom) polyclonal T cells *in vitro*, activated through OKT3/CD28. TCR Vβ1 staining is shown in total $CD3^+$, $CD3^+/CD4^+$, $CD3^+/CD8^+$ cells, whereas SLL-dextramer$^+$ staining is shown in total $CD3^+$ and in SLL-dextramer–sorted T cells (postsorting). **C,** The average of the positive TCR Vβ1 cells was shown in total $CD3^+$, $CD3^+$ $CD8^+$, and $CD3^+$ $CD4^+$ T cells, whereas the average of positive SLL-textramer cells was shown in $CD3^+$ $CD8^+$ and $CD3^+$ $CD4^+$ T cells. Data are expressed as average ± SD from 8 healthy donors at day 15 of *in vitro* expansion. **D,** Fold expansion of untransduced T cell (CNT, gray dashed line) and iC9-SLL TCR T cell (black line), evaluated by Trypan blue count assay. Data represent results from 8 healthy donors.

Published OnlineFirst April 3, 2018; DOI: 10.1158/0008-5472.CAN-17-3140

for CD8$^+$ cells (Fig. 2B). Indeed, no significant differences in the transduction level or iC9-SLL TCR pairing investigated by dextramer staining analysis were observed between total mononuclear cells and CD8$^+$ selected T cells. Moreover, to enrich the T-cell population that express the correct SLL-TCR chain pairing, we also performed a microbeads-positive selection of genetically modified T cells stained with SLL-dextramer, showing that the selected SLL-TCR$^+$ T cells were capable to stably express the transgene (Fig. 2B) and to expand. Although iC9-SLL TCR T cells are characterized by the expression of TCRVβ1, SLL-TCR$^+$ T cells remain polyclonal after transduction, as no preferential TCRβ family usage has been observed in SLL-dextramer$^+$ T cells beside SLL-specific Vβ1 (Supplementary Fig. S7). Transduced T cells maintained their ability to proliferate at the same level of nontransduced T cells (CNT T cells) when exposed to the pleiotropic cytokine IL2 (10.7±7.6 and 17.5±16.5-fold expansion at day 15, respectively, Fig. 2D). The ectopically expressed SLL TCR was functional, as iC9-SLL TCR T cells produce IFNγ in response to the CEM-T2 cell line loaded with the SLL peptide (until 10^{-5} mol/L concentration), but not with the irrelevant PRAME-peptide ALY (Fig. 3A). iC9-SLL TCR T cells also lysed SLL peptide-pulsed CEM-T2 cells at higher extent than un-loaded CEM-T2 (i.e., a HLA-A*02+ cell line characterized by low PRAME expression, as shown in Supplementary Fig. S8A; 69.8%±6.5% vs. 8.0%±1.8% specific lysis, respectively, at the effector:target (E:T) ratio of 20:1, Fig. 3B). Moreover, in coculture experiments, iC9-SLL TCR T cells were able to eliminate the tumor cell line U266 (HLA-A02$^+$ PRAME$^+$) without the need of a SLL-peptide preloading (Supplementary Fig. S8C).

As previously mentioned, to improve in a clinical perspective the safety of our transduced T cells, we included in the retroviral vector the iC9-suicide gene. Functional experiments demonstrated that also the second transgene is active, as iC9-SLL TCR T cells were promptly eliminated upon 24-hour exposure to 20 nmol/L AP1903 (Fig. 3C). The residual CD3$^+$ Vβ1$^+$ cells (average, 6.3%±3.9%) still alive after 72 hours of AP1903 exposure were further expanded in culture with IL2, and tested for the presence of vector DNA, showing the absence of genetically modified T cells (Fig. 3D).

PRAME-specific TCR-redirected T cells exert antitumor activity toward HLA-A*02–matched medulloblastoma cell line

We evaluated the cytotoxic activity of iC9-SLL TCR T cells using standard 6-hour ^{51}Cr release assays against the HLA-A*02$^+$ PRAME$^+$ MB DAOY cell line and a negative control, namely the HLA-A*02neg.ve PRAME$^+$ RS4;11 cell line (Supplementary Fig. S8). We demonstrated that iC9-SLL TCR T cells produced significantly greater lysis of the HLA-A*02$^+$ PRAME$^+$ medulloblastoma cell line DAOY (43.3%±17.7% specific lysis at the E:T ratio of

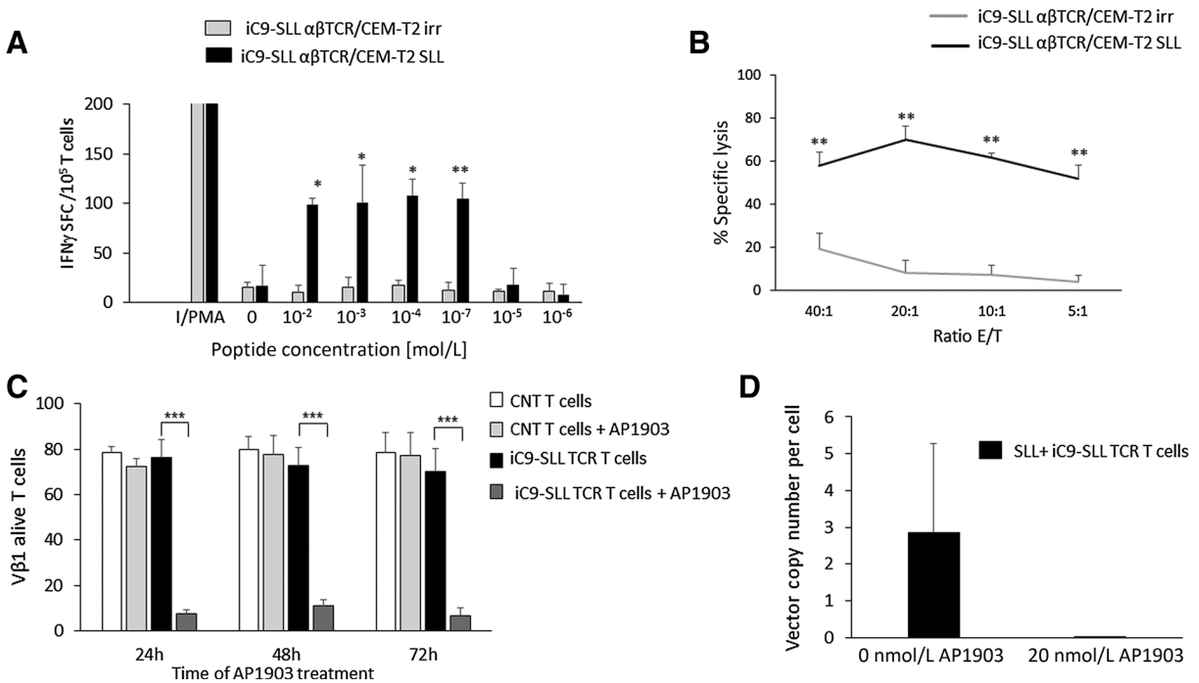

Figure 3.

In vitro functional analysis of iC9-SLL TCR T cells. **A,** iC9-SLL TCR avidity assessed by IFNγ ELISpot assays of CEM-T2 cell line loaded with an irrelevant peptide (gray bars) and the SLL-specific peptide (black bars). Ionomycin/phorbol myristate acetate (I/PMA) was used as positive control. SFCs per 10^5 cells. Data represent the mean ± SD of triplicate experiments. **B,** *In vitro* ^{51}Cr release assay evaluating cytolytic activity of iC9-SLL TCR T cells on CEM-T2 tumor cell line loaded with an irrelevant (irr; gray line) or SLL-specific peptide (black line). **C,** Evaluation of percentage of alive (Annexin-V$^-$/7AAD$^-$) T cells grown in IL2 and exposed to 20 nmol/L AP1903 for 24, 48, or 72 hours. CD3$^+$ TCR Vβ1$^+$ T cells negative for Annexin-V/7AAD staining were considered to be alive after the activation of the iC9 suicide gene. Data from four healthy donors are expressed as average ± SD. **D,** Analysis of the presence of retroviral vector sequence in iC9-SLL TCR T cells residual after AP1903 exposition. Quantitative PCR targeting specific retroviral sequence was carried out to establish whether Vβ1$^+$ T cells residual after AP1903 exposition were genetically modified. Data from three independent experiments show that Vβ1$^+$ residual cells did not carry iC9-SLL TCR vector. *, $P \leq 0.05$; **, $P \leq 0.01$; ***, $P \leq 0.001$.

Published OnlineFirst April 3, 2018; DOI: 10.1158/0008-5472.CAN-17-3140

20:1) than that observed with CNT T cells (11.3%±6.1%; $P = 0.004$; Supplementary Fig. S8B). Moreover, no significant differences were observed in cytotoxic activity between iC9-SLL TCR bulk T cells (Supplementary Fig. S8D) or iC9-SLL TCR CD8$^+$ T cells (40.4%±15% specific lysis at the E:T ratio of 20:1; Supplementary Fig. S8E). In contrast, we observed negligible killing for both transduced and control T cells against the control target HLA-A*02neg.ve PRAME$^+$ RS4;11 cell line (Supplementary Fig. S8F). In longer-term assays, in which we cocultured control or iC9-SLL TCR T cells with HLA-A*02$^+$ PRAME$^+$ DAOY cells for 7 days, we found a significant reduction of DAOY tumor cells in the presence of iC9-SLL TCR T cells at E:T ratio of 1:1 (Fig. 4A and B). To obtain similar results also on D283 cell line characterized by downregulation of the HLA-A*02 molecule (Supplementary Fig. S8B), we needed to pretreat target cells with IFNγ for 48 hours (Fig. 4A). The cytotoxic effect was paralleled by IFNγ production by iC9-SLL TCR T cells against medulloblastoma cell lines as assessed by ELISA assays (Fig. 4C). Moreover, we sought to evaluate whether SLL$^+$ sorted T cells were still able to be functional toward HLA-A*02$^+$ PRAME$^+$ DAOY cells. In particular, tumor control was mediated by the CD8$^+$ Vβ1$^+$ T-cell subpopulation, whereas neither antigen-specific proliferation (Supplementary Figs. S9 S10A and S10B), nor a direct antitumor activity (Fig. 4B), as well as cytokine production, evaluated in terms of IFNγ (Fig. 4C), IL2 (Supplementary Fig. S10C), and TNFα (Supplementary Fig. S10D), was observed when CD4$^+$ Vβ1$^+$ T cells were used as effector cells. To strengthen our findings, we also sought to evaluate whether iC9-SLL TCR T cells were activated by primary HLA-A*02$^+$ medulloblastoma cells derived from patient with medulloblastoma (#1). These cells were *in vitro* expanded until passage 5 and were confirmed to maintain both high PRAME expression (Supplementary Fig. S11) and other neuronal markers, including B3TUBB, S100A, and GFAP. We observed a significant increase in IFNγ SFC T cells, when iC9-SLL TCR T cells were challenged with HLA-A*02+ MB #1 cells, irrespective of pretreatment with IFNγ, with respect to the control condition (CNT T cells; $P = 0.004$). Negligible activity was detected when iC9-SLL TCR T cells were stimulated in the presence of PRAME$^+$ HLA-A*02$^-$ MB #2 and #3 primary tumor cells (Fig. 4D).

iC9-SLL TCR T cells exert antitumor activity *in vivo* in xenogeneic mouse models of medulloblastoma

To confirm *in vivo* the antitumor function of iC9-SLL TCR$^+$ T cells, we first used xenogeneic NSG mouse models

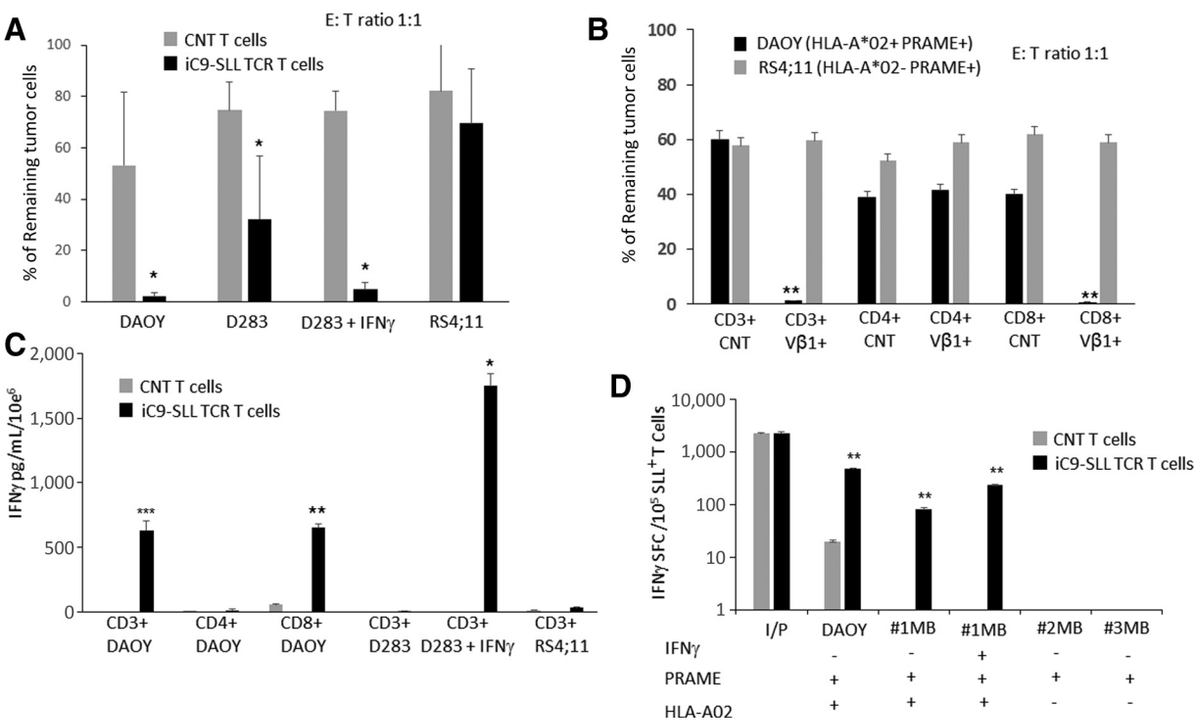

Figure 4.

Long-term *in vitro* functional analysis of iC9-SLL TCR T cells against medulloblastoma cell lines and primary patient-derived tumor cells. **A,** Seven-day coculture assay between effector cells [control CNT T cells (gray bars) or iC9-SLL TCR T cells (black bars)] and PRAME$^+$ HLA-A*02$^+$ medulloblastoma cell line DAOY, PRAME$^+$ medulloblastoma cell line D283 downregulating HLA Class I molecule, D283 cell line pretreated with IFNγ (1,000 U/mL) for 48 hours, and PRAME$^+$ HLA-A*02- RS4;11 cell line (1:1 E:T ratio). Data are expressed as average ± SD from three healthy donors. **B,** Seven-day coculture assay (1:1 E:T ratio) between PRAME$^+$ HLA-A*02$^+$ MB cell line DAOY (black bars) or PRAME$^+$ HLA-A*02- RS4;11 cell line (gray bars) and effector cells (control CNT T cells or Vβ1+ iC9-SLL TCR T cells) sorted in the subset of CD3$^+$, CD3$^+$ CD4$^+$, and CD3$^+$ CD8$^+$ T cells. Data are expressed as average ± SD from three healthy donors. **C,** IFNγ quantification by ELISA assay of supernatant after 24 hours of coculture assay described in **A** and **B**. *, $P \leq 0.05$; **, $P \leq 0.01$; ***, $P \leq 0.001$. **D,** IFNγ ELISpot assays of untransduced CNT T cells (gray bars) or iC9-SLL$^+$ TCR T cells (black bars) challenged with primary medulloblastoma cells derived from patient with PRAME$^+$ HLA-A02$^+$ (#1) with or w/out IFNγ pretreatment, or patients with PRAME$^+$ HLA-A02$^-$ (#2 and #3). SFCs per 10^5 cells. Data represent the average ± SD of triplicate experiments (*, $P \leq 0.05$; **, $P \leq 0.01$).

Published OnlineFirst April 3, 2018; DOI: 10.1158/0008-5472.CAN-17-3140

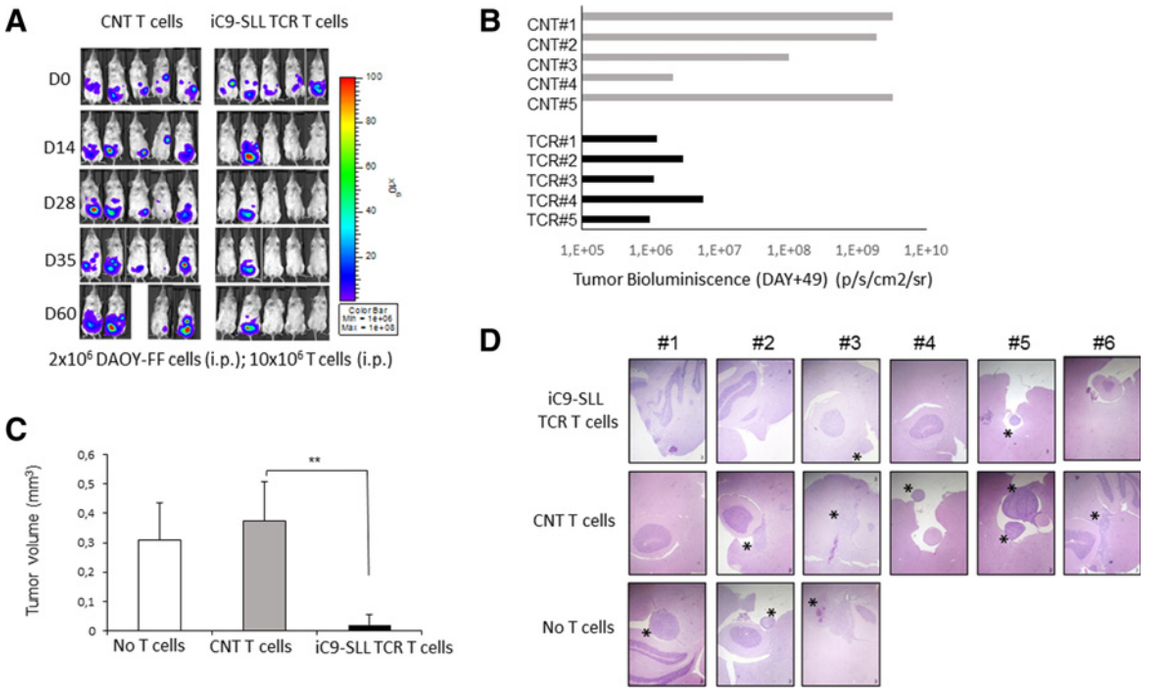

Figure 5.

iC9-SLL TCR T cells have *in vivo* antitumor activity against DAOY cell line. **A** and **B,** Intraperitoneal administration of 2×10^6 DAOY-FFluc cells into NSG mice ($n = 10$), followed by T-cell infusions [10^7; 5 mice with untransduced (CNT) and 5 mice with iC9-SLL TCR T cells] and weekly BLI. BLI in individual mice from both treatment groups at day +49 from T-cell infusion is shown in **B**. Scale, 1×10^6 to 1×10^8 photons/second/cm^2/sr. **C** and **D,** Stereotaxical administration of 2×10^5 DAOY cells into NSG mice ($n = 15$), followed by intratumor infusions of placebo (PBS, No T cells; $n = 3$), untransduced (CNT; $n = 6$; 10^7) or iC9-SLL TCR T cells ($n = 6$; 10^7). After 4 weeks, animals were sacrificed and brains were evaluated for histopathologic H&E analysis by serial section of the cerebellum. Tumor area (marked by asterisk where observed) of every slice was evaluated with a microscope, and average ± SD of tumor volumes is shown in **C**, whereas exemplificative slide section (magnification, ×4) of the cerebella is shown in **D** (*, $P \leq 0.05$; **, $P \leq 0.001$).

intraperitoneally engrafted in Matrigel with a bulky medulloblastoma tumor, represented by DAOY cells (2×10^6) genetically modified with firefly luciferase (FFLuc), to monitor tumor growth overtime by bioluminescent imaging (BLI) (Supplementary Fig. S12A). After establishment of bulky tumor (i.e., 20 days after DAOY intraperitoneal injection), mice were treated with either control (CNT) or iC9-SLL TCR T cells (Fig. 5A). On day 60 after T-cell infusion, 4 of 5 mice treated with iC9-SLL TCR T cells had significantly better control of tumor growth than mice receiving CNT T cells ($6.4 \times 10^6 \pm 10 \times 10^6$ vs. $11{,}300 \times 10^6 \pm 8010 \times 10^6$ photons/second; respectively; $P = 0.03$, Fig. 5A and B). To obtain further evidence of the iC9-SLL αβTCR T-cell antitumor activity, we developed an orthotopic medulloblastoma mouse model where DAOY cells (2×10^5) are stereotaxically implanted into the cerebellum (Supplementary Fig. S12B and 12C). After 10 days, mice were divided in three cohorts, receiving further stereotaxic surgery to infuse placebo (namely, no T cells; $n = 3$), control T cells (namely, CNT T cells; $n = 6$) and T cells genetically modified with iC9-SLL TCR (namely, iC9-SLL TCR T cells; $n = 6$). On day +40, mice were sacrificed and cerebella surgically excised. Histopathologic analysis showed tumor presence in a significantly lower percentage of mice receiving iC9-SLL TCR T cells as compared with controls (2/6 vs. 6/6, respectively). In addition, tumor volume analysis (calculated along serial histologic brain sections as described previously; ref. 28) displayed a significant reduction of the tumor mass formed by DAOY cells in iC9-SLL TCR T-cell–treated mice as compared with controls (Fig. 5C and D). We were also able to observe a significant reduction of the tumor volume when iC9-SLL TCR T cells were administered by intravenous infusion (Fig. 6A and B). To better demonstrate that tumor eradication is a direct consequence of the T-cell migration across the blood–brain barrier (BBB), we sacrificed mice and performed anti-hCD3 IHC analysis on brain slides. Human T cells colocalized together with medulloblastoma cells, while a negligible human T-cell infiltrate was seen in mouse brain sites not involved by the tumor (Fig. 6C).

As medulloblastoma phenomena could represent a life-threatening effect in our system, we have also studied the kinetics of tumor elimination when medulloblastoma cell line (marked with FF-Luc) was intracranially implanted and T cells were injected intravenously. As shown in Fig. 6D, tumor eradication was obtained in 15 days from T-cell infusion in the cohort of mice receiving iC9-SLL TCR T cells, this translating into a significant improvement of mice OS (Fig. 6E). No neurologic signs of toxicity were also recorded after iC9-SLL TCR T-cell infusion, by applying comprehensive behavioral assessment involving a battery of 33 semiquantitative tests for general health and sensory function, baseline behaviors, and neurologic reflexes included in Supplementary Table S1; ref. 25).

To verify the effectiveness of iC9 activation also in T cells infiltrating the cerebellum, we genetically modified iC9-SLL TCR

Published OnlineFirst April 3, 2018; DOI: 10.1158/0008-5472.CAN-17-3140

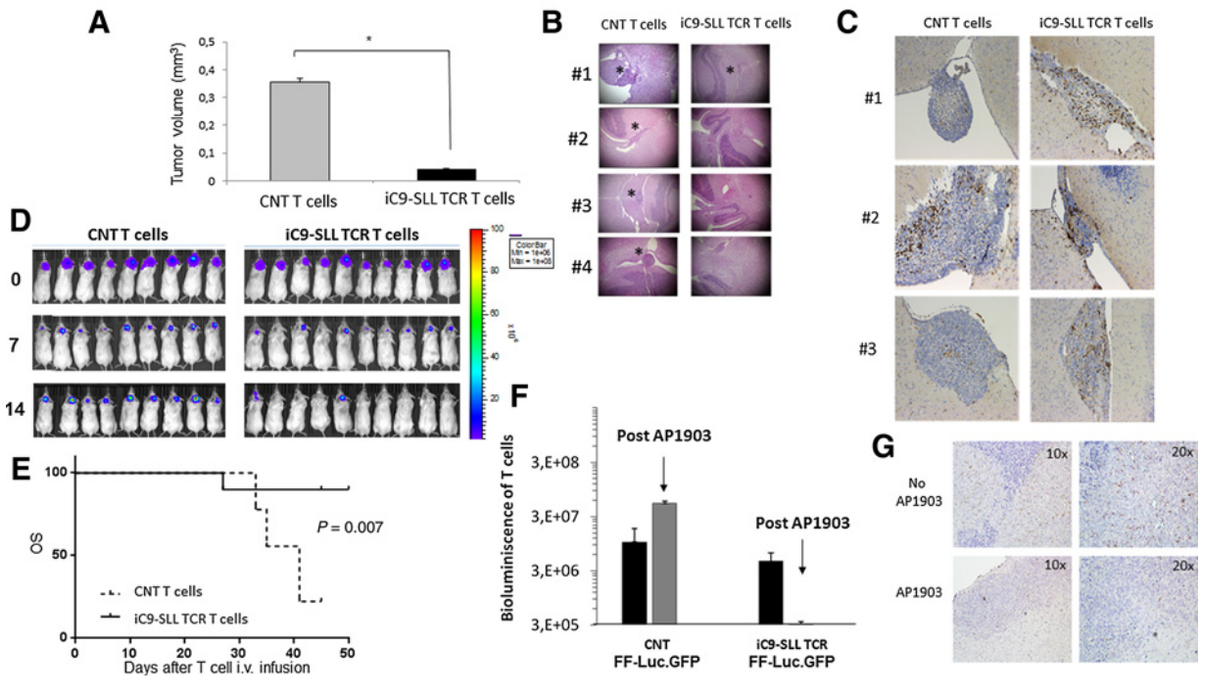

Figure 6.

iC9-SLL TCR T cells infused systemically have *in vivo* antitumor activity against orthotopic DAOY cell line implant. **A–C,** Mice stereotaxically implanted with DAOY were infused intravenously ($n = 8$) into the tail vein with untransduced (CNT; $n = 4$; 10^7) or iC9-SLL TCR T cells ($n = 4$; 10^7). Tumor area (marked by asterisk where observed) of every slice was evaluated with a microscope, and average ± SD of tumor volumes is shown in **A**, whereas exemplificative slide section (magnification, ×4) of the cerebella is shown in **B**. **C,** Tumor T-cell infiltrates were analyzed by anti-hCD3 IHC on cerebella slides of mice sacrificed after 5 days from T-cell intravenous infusion. **D** and **E,** The dynamics of tumor regression after tail vein injection of untransduced (CNT; $n = 9$; 10^7) or iC9-SLL TCR T cells ($n = 9$; 10^7) was also evaluated, applying BLI in the orthotopic mouse model implanted with DAOY cell line genetically modified with FF-luc vector ($n = 18$) (**D**). **E,** After the tumor clearance (by 14 days after iC9-SLL TCR T-cell infusion), mice were evaluated for OS until day 45 (end of the experiment). **F** and **G,** Mice stereotaxically implanted with WT DAOY were infused intravenously ($n = 8$) into the tail vein control (CNT; $n = 4$; 10^7) or dextramer-sorted iC9-SLL TCR T cells ($n = 4$; 10^7) also genetically modified with FF-Luc vector. At day +4 after T-cell infusion, all the mice were evaluated for BLI (black bars), and two mice in each cohort received intraperitoneal administration of 100 mg/mouse of the dimerizing AP1903 for two consecutive days. After additional 24 hours, all the mice were reevaluated for BLI (gray bars) and thereafter sacrificed. **G,** Tumor T-cell infiltrates were analyzed by anti-hCD3 IHC on cerebella slides of mice treated with iC9-SLL TCR T cells in the absence (top) or treated with AP1903 (bottom). The use of a systemically administration of AP1903 corresponded to a significant reduction of tumor T-cell infiltration.

T cells with a retroviral vector carrying the FireFly Luciferase to follow their *in vivo* elimination upon the intravenous administration of AP1903. As shown by Fig. 6F, the systemic administration of the dimerizing drug allows a significant reduction of the BLI in the mouse cohort receiving iC9-SLL TCR T cells, but not in mice infused with CNT T cells. Moreover, anti-hCD3 IHC analysis on cerebella slides of mice treated with iC9-SLL TCR T cells shows that the administration of AP1903 completely eliminates tumor T-cell infiltration (Fig. 6G).

Discussion

Medulloblastoma is the most common, highly aggressive, central nervous tumor of childhood and remains a challenging disease to treat. This study shows that adoptive immunotherapy with T cells redirected toward PRAME antigen could represent an innovative therapeutic approach for this neoplasm. Indeed, CTAs such as PRAME are considered a promising target for immunotherapy, because of their limited expression in normal tissues (except the testis, which, however, has no expression of human leukocyte antigen molecules; ref. 29). Several authors reported PRAME expression in many cancers, but currently the biological and clinical meaning of this finding is not yet completely elucidated and, in some cases, the association between PRAME expression and disease prognosis is controversial. (30–32) In particular, in solid malignancies, including head and neck cancer, (33, 34) liposarcoma,(35) uveal melanoma, (12, 36) osteosarcoma, (37, 38) breast cancer (39), and neuroblastoma (40) high PRAME expression correlates with advanced stage disease and poor clinical outcome, whereas in pediatric acute leukemia, PRAME overexpression was found to predict good outcome (41, 42).

The expression of PRAME in medulloblastoma has been previously evaluated and reported in gene expression datasets and publications (6, 7) as having no correlation with patient clinical outcome. (6) We investigated the expression levels of the PRAME antigen in patients with medulloblastoma, finding that 82% of samples had PRAME mRNA expression levels higher than those of normal adult cerebellum. By applying a maximum-likelihood analysis statistical tool, we defined a PRAME expression cutoff able to subdivide patients into two categories, namely patients with high (19 of 51, 37%) and low

Published OnlineFirst April 3, 2018; DOI: 10.1158/0008-5472.CAN-17-3140

PRAME-expression. A low expression of PRAME correlated with a better 5-year OS probability, a finding similar to that observed in other cancers. (33, 36, 39, 40) Moreover, the correlation between better OS and low PRAME expression was detected in patients belonging to SHH- and G3-MB subgroups, while a larger number of patients is needed to confirm this finding in WNT- and G4-MB subgroups. The statistically significant correlation between low PRAME expression and better OS probability was also maintained considering as cutoff for PRAME mRNA expression median value, as well as 1° and 3° quartiles.

The high expression of PRAME in most patients with medulloblastoma and its persistence in recurrent disease samples provide the rationale for considering this CTA a promising candidate for targeted immunotherapies. Indeed, PRAME has already been evaluated, both *in vitro* (8, 10) and *in vivo*, for its immunogenicity. In particular, PRAME has been reported to induce CTL-mediated immune responses in melanoma and in acute/chronic leukemia, (43) and, thus, represents a promising target for TAA-specific immune therapies. This CTA has been recently exploited as immunotarget in several vaccination trials, as full-length protein/peptides either alone or in combination with a different tumor antigen. In particular, PRAME-based immunotherapy had an acceptable safety profile and induced anti-PRAME-specific humoral and cellular immune responses in melanoma (44, 45), as well as in non–small cell lung cancer, (46) prostate carcinoma, and renal clear cell carcinoma. (45)

The vaccination approaches using PRAME as target, however, clearly showed the difficulty of *in vivo* reactivating PRAME-specific $CD8^+$ T cells, even after several consecutive rounds of administration of the immunogenic protein/peptides. In light of this observation, we sought to exploit the relevance of PRAME as target for adoptive TCR T-cell therapy with an alternative approach, namely that of T cells genetically modified to express a high-affinity TCR, specific for the PRAME-derived peptide SLL. This peptide is presented in the context of HLA-A*02, which has a high worldwide frequency (i.e., 48.4% and 22.6% on average for Caucasian and Black ethnic groups, respectively; ref. 47). In particular, this PRAME-specific TCR, derived from the allogeneic HLA repertoire, was selected in view of its high avidity for the cognate peptide, high reactivity against several HLA-A*02 positive PRAME-expressing tumor cell lines, as well as freshly isolated metastatic melanoma and primary leukemia cells. Moreover, no reactivity was reported when genetically modified T cells were challenged against a large panel of nonmalignant cells, including either fresh or activated B cells, T cells, MØ1 and MØ2 macrophages, CD34 cells, immature dendritic cells (DC) derived from either $CD34^+$ or $CD14^+$ cells. The T-cell clone from which SLL-TCR was derived exerted limited on-target reactivity against kidney epithelial cells and mature DCs (mDC). However, the reactivity against the latter may be beneficial, as professional APCs like mDCs may contribute to enhance antitumor response and persistence of the infused T cells (11). In this study, we chose to evaluate the antitumor activity of PRAME-specific allo-TCR against medulloblastoma cells. In addition, the iC9 safety switch was introduced with the aim of increasing the clinical safety of our modified PRAME-TCR product. Notably, iC9-SLL TCR T cells will be evaluated in an ongoing phase I trial recruiting patients with either relapsed or refractory myeloid neoplasms (ClinicalTrials.gov Identifier NCT02743611).

To date, iC9 is one of the most promising suicide genes for several reasons, including limited immunogenicity (13) and prompt activity, as more than 99% iC9-expressing T cells (iC9-T cells) are eliminated both *in vitro* and *in vivo* within 2 hours from the administration of a single dose of the prodrug AP1903 (rimiducid, a synthetic and nontoxic ligand leading to iC9 dimerization and triggering of the apoptotic pathway; refs. 48, 49). Indeed, iC9 activation alone has been shown to produce rapid and sustained control of graft-versus-host disease caused by donor-derived iC9-T cells in recipients of allogeneic stem cell transplantation (48–51).

To the best of our knowledge, no data were available on the possibility to use iC9 suicide gene system also to control the presence of genetically modified cells in the brain compartment. In this work, we have proven that the systemic administration of the dimerizing drug AP1903 in a medulloblastoma orthotopic mouse model led to both BLI reduction in the total mouse body, including brain, and the lack of $hCD3^+$ T cells in mouse cerebellum.

We formally proved that both transgenes in the construct (namely, SLL-TCR and iC9) are functionally active and iC9-SLL TCR T cells, in particular the $CD8^+$ T-cell subset, exert cytotoxic activity toward DAOY cells, as well as D283 cells in which we reestablished HLA expression by IFNγ treatment. IFNs have been used clinically to treat a variety of malignancies, protecting against disease by direct effects on target cells and by activating immune responses (52). These results support the use of IFNs to boost an adoptive T-cell therapy based on HLA-mediated target recognition. Importantly, despite the relevant difficulty to collect tumor material from patients with medulloblastoma, we were able to challenge iC9-SLL TCR^+ T cells with primary medulloblastoma cells derived from the biopsy of one patient whose tumor cells were HLA-A*02+ and PRAME+, and two patients characterized HLA-A*02neg.ve and $PRAME^+$ tumor cells, by showing a significant PRAME specific T-cell activation only in patient with HLA-A*02^+. A larger cohort of primary medulloblastoma tissues needs to be evaluated to further corroborate this finding.

In vivo animal models confirmed the *in vitro* observations, showing that medulloblastoma cells are a suitable target for adoptive TCR T-cell therapy, regardless of the need of HLA upregulation by IFNγ administration. A significant tumor control in the absence of undue toxicity was documented when both DAOY cells and iC9-SLL TCR T cells were injected through a stereotaxic approach in the mouse cerebellum. When T cells were infused intravenously, we also demonstrated tumor control, coupled with T-cell infiltration of the tumor tissue and improved OS. This relevant model proving iC9-SLL TCR T-cell activity was not associated to any neurologic sign of sufferance in the treated mice. These findings provide experimental support to the hypothesis that systemic administration of iC9-SLL TCR T cells could be a suitable and safe approach, particularly in view of T-cell migration across the BBB.

In conclusion, this study shows that iC9-SLL TCR T cells are capable of killing medulloblastoma cells and might represent an innovative, effective strategy leading to a significant improvement of the outcome of patients with medulloblastoma. This novel form of immunotherapy should be tested in early-phase clinical trials for patients with medulloblastoma with either relapsed or newly diagnosed disease, but with features predicting a high risk of treatment failure.

Published OnlineFirst April 3, 2018; DOI: 10.1158/0008-5472.CAN-17-3140

Disclosure of Potential Conflicts of Interest

M.H.M. Heemskerk has ownership interest (including patents) in a U.S. patent (US Serial No. 62/130,884, filed March 10, 2015, entitled "T-Cell Receptors Directed Against the Preferentially Expressed Antigen of Melanoma and Uses Thereof"). No potential conflicts of interest were disclosed by the other authors.

Authors' Contributions

Conception and design: E. Miele, B.D. Angelis, A. Moseley, E. Ferretti, F. Locatelli, C. Quintarelli

Development of methodology: E. Miele, B.D. Angelis, I. Caruana, A. Camera, A. Moseley, C. Quintarelli

Acquisition of data (provided animals, acquired and managed patients, provided facilities, etc.): E. Miele, B.D. Angelis, M. Guercio, M. Sinibaldi, I. Caruana, L. Abballe, A. Carai, A. Camera, F. Giangaspero, A. Mastronuzzi, C. Quintarelli

Analysis and interpretation of data (e.g., statistical analysis, biostatistics, computational analysis): D. Orlando, E. Miele, B.D. Angelis, I. Boffa, E. Ferretti, F. Locatelli, C. Quintarelli

Writing, review, and/or revision of the manuscript: D. Orlando, E. Miele, B.D. Angelis, I. Caruana, S. Caruso, M.H.M. Heemskerk, A. Mastronuzzi, E. Ferretti, F. Locatelli, C. Quintarelli

Administrative, technical, or material support (i.e., reporting or organizing data, constructing databases): D. Orlando, E. Miele, B.D. Angelis, M. Guercio, I. Boffa, I. Caruana, R.S. Hagedoorn, M.H.M. Heemskerk

Study supervision: E. Ferretti, F. Locatelli, C. Quintarelli

Other (performed *in vivo* experiments): A. Po

Acknowledgments

The work was partly supported by grants from Italian Ministry of Health (RF-2010-2316606 to F. Locatelli; GR-2013-02359212 to C. Quintarelli); AIRC (Associazione Italiana Ricerca sul Cancro, Special Grant "5xmille"-9962 and Investigator Grant 2015 to F. Locatelli; Start-up 2015 grant; to I. Caruana), Ricerca Corrente (2017; grant to C. Quintarelli, B. De Angelis, I. Caruana); Fondazione Neuroblastoma (to F. Locatelli); Istituto Giuseppe Toniolo di Studi Superiori (to A. Mastronuzzi and M. Guercio), Associazione Heal onlus (to A. Mastronuzzi). We would like to thank Bellicum Pharmaceuticals for kindly providing AP1903. We thank Ezio Giorda, Marco Pezzullo, Marco Scarsella and Cristiano De Stefanis core facilities, Bambino Gesù Children's Hospital, Rome, Italy, for the technical advice and experimental support.

The costs of publication of this article were defrayed in part by the payment of page charges. This article must therefore be hereby marked *advertisement* in accordance with 18 U.S.C. Section 1734 solely to indicate this fact.

Received October 12, 2017; revised February 16, 2018; accepted March 30, 2018; published first April 3, 2018.

References

1. Martin AM, Raabe E, Eberhart C, Cohen KJ. Management of pediatric and adult patients with medulloblastoma. Curr Treat Options Oncol 2014;15:581–94
2. Packer RJ, Gajjar A, Vezina G, Rorke-Adams L, Burger PC, Robertson PL, et al. Phase III study of craniospinal radiation therapy followed by adjuvant chemotherapy for newly diagnosed average-risk medulloblastoma. J Clin Oncol 2006;24:4202–8
3. Packer RJ, Sutton LN, Elterman R, Lange B, Goldwein J, Nicholson HS, et al. Outcome for children with medulloblastoma treated with radiation and cisplatin, CCNU, and vincristine chemotherapy. J Neurosurg 1994;81:690–8
4. Ikeda H, Lethe B, Lehmann F, van Baren N, Baurain JF, de Smet C, et al. Characterization of an antigen that is recognized on a melanoma showing partial HLA loss by CTL expressing an NK inhibitory receptor. Immunity 1997;6:199–208.
5. Wadelin F, Fulton J, McEwan PA, Spriggs KA, Emsley J, Heery DM. Leucine-rich repeat protein PRAME: expression, potential functions and clinical implications for leukaemia. Mol Cancer 2010;9:226
6. Vulcani-Freitas TM, Saba-Silva N, Cappellano A, Cavalheiro S, Toledo SR. PRAME gene expression profile in medulloblastoma. Arq Neuropsiquiatr 2011;69:9–12.
7. Boon K, Edwards JB, Siu IM, Olschner D, Eberhart CG, Marra MA, et al. Comparison of medulloblastoma and normal neural transcriptomes identifies a restricted set of activated genes. Oncogene 2003;22:7687–94
8. Quintarelli C, Dotti G, De Angelis B, Hoyos V, Mims M, Luciano L, et al. Cytotoxic T lymphocytes directed to the preferentially expressed antigen of melanoma (PRAME) target chronic myeloid leukemia. Blood 2008;112:1876–85
9. Kessler JH, Beekman NJ, Bres-Vloemans SA, Verdijk P, van Veelen PA, Kloosterman-Joosten AM, et al. Efficient identification of novel HLA-A(*)0201-presented cytotoxic T lymphocyte epitopes in the widely expressed tumor antigen PRAME by proteasome-mediated digestion analysis. J Exp Med 2001;193:73–88.
10. Quintarelli C, Dotti G, Hasan ST, De Angelis B, Hoyos V, Errichiello S, et al. High-avidity cytotoxic T lymphocytes specific for a new PRAME-derived peptide can target leukemic and leukemic-precursor cells. Blood 2011;117:3353–62
11. Amir AL, van der Steen DM, van Loenen MM, Hagedoorn RS, de Boer R, Kester MD, et al. PRAME-specific Allo-HLA-restricted T cells with potent antitumor reactivity useful for therapeutic T-cell receptor gene transfer. Clin Cancer Res 2011;17:5615–25
12. Gezgin G, Luk SJ, Cao J, Dogrusoz M, van der Steen DM, Hagedoorn RS, et al. PRAME as a potential target for immunotherapy in metastatic uveal melanoma. JAMA Ophthalmol 2017;135:541–9.
13. Straathof KC, Pule MA, Yotnda P, Dotti G, Vanin EF, Brenner MK, et al. An inducible caspase 9 safety switch for T-cell therapy. Blood 2005;105:4247–54
14. Gargett T, Brown MP. The inducible caspase-9 suicide gene system as a "safety switch" to limit on-target, off-tumor toxicities of chimeric antigen receptor T cells. Front Pharmacol 2014;5:235
15. Louis DN, Perry A, Burger P, Ellison DW, Reifenberger G, von Deimling A, et al. International Society Of Neuropathology–Haarlem consensus guidelines for nervous system tumor classification and grading. Brain Pathol 2014;24:429–35
16. Louis DN, Perry A, Reifenberger G, von Deimling A, Figarella-Branger D, Cavenee WK, et al. The 2016 World Health Organization Classification of Tumors of the Central Nervous System: a summary. Acta Neuropathol 2016;131:803–20
17. Vera J, Savoldo B, Vigouroux S, Biagi E, Pule M, Rossig C, et al. T lymphocytes redirected against the kappa light chain of human immunoglobulin efficiently kill mature B lymphocyte-derived malignant cells. Blood 2006;108:3890–7
18. Quintarelli C, Vera JF, Savoldo B, Giordano Attianese GM, Pule M, Foster AE, et al. Co-expression of cytokine and suicide genes to enhance the activity and safety of tumor-specific cytotoxic T lymphocytes. Blood 2007;110:2793–802
19. Ferretti E, De Smaele E, Miele E, Laneve P, Po A, Pelloni M, et al. Concerted microRNA control of Hedgehog signalling in cerebellar neuronal progenitor and tumour cells. EMBO J 2008;27:2616–27
20. Ferretti E, De Smaele E, Po A, Di Marcotullio L, Tosi E, Espinola MS, et al. MicroRNA profiling in human medulloblastoma. Int J Cancer 2009;124:568–77
21. Miele E, Mastronuzzi A, Po A, Carai A, Alfano V, Serra A, et al. Characterization of medulloblastoma in Fanconi Anemia: a novel mutation in the BRCA2 gene and SHH molecular subgroup. Biomark Res 2015;3:13
22. Northcott PA, Shih DJ, Remke M, Cho YJ, Kool M, Hawkins C, et al. Rapid, reliable, and reproducible molecular sub-grouping of clinical medulloblastoma samples. Acta Neuropathol 2012;123:615–26
23. Livak KJ, Schmittgen TD. Analysis of relative gene expression data using real-time quantitative PCR and the 2(-Delta Delta C(T)) Method. Methods 2001;25:402–8

24. Di Stasi A, De Angelis B, Savoldo B. Gene therapy to improve migration of T cells to the tumor site. Methods Mol Biol 2010;651:103–18
25. Wilson KD, Stutz SJ, Ochoa LF, Valbuena GA, Cravens PD, Dineley KT, et al. Behavioural and neurological symptoms accompanied by cellular neuroinflammation in IL-10-deficient mice infected with *Plasmodiumchabaudi*. Malar J 2016;15:428
26. Smits M, van Rijn S, Hulleman E, Biesmans D, van Vuurden DG, Kool M, et al. EZH2-regulated DAB2IP is a medulloblastoma tumor suppressor and a positive marker for survival. Clin Cancer Res 2012;18:4048–58
27. Grizzi F, Franceschini B, Hermonat PL, Liu Y, Chiriva-Internati M. Some remarks on the somatic expression of sperm protein 17. Int J Cancer 2004;111:972–3.
28. Infante P, Mori M, Alfonsi R, Ghirga F, Aiello F, Toscano S, et al. Gli1/DNA interaction is a druggable target for Hedgehog-dependent tumors. EMBO J 2015;34:200–17
29. Hermes N, Kewitz S, Staege MS. Preferentially expressed antigen in melanoma (PRAME) and the PRAME family of leucine-rich repeat proteins. Curr Cancer Drug Targets 2016;16:400–14.
30. Tajeddine N, Louis M, Vermylen C, Gala JL, Tombal B, Gailly P. Tumor associated antigen PRAME is a marker of favorable prognosis in childhood acute myeloid leukemia patients and modifies the expression of S100A4, Hsp 27, p21, IL-8 and IGFBP-2 in vitro and in vivo. Leukemia Lymphoma 2008;49:1123–31
31. Sun Z, Wu Z, Zhang F, Guo Q, Li L, Li K, et al. PRAME is critical for breast cancer growth and metastasis. Gene 2016;594:160–4
32. Damm F, Heuser M, Morgan M, Wagner K, Gorlich K, Grosshennig A, et al. Integrative prognostic risk score in acute myeloid leukemia with normal karyotype. Blood 2011;117:4561–8
33. Szczepanski MJ, DeLeo AB, Luczak M, Molinska-Glura M, Misiak J, Szarzynska B, et al. PRAME expression in head and neck cancer correlates with markers of poor prognosis and might help in selecting candidates for retinoid chemoprevention in pre-malignant lesions. Oral Oncol 2013; 49:144–51
34. Szczepanski MJ, Whiteside TL. Elevated PRAME expression: what does this mean for treatment of head and neck squamous cell carcinoma? Biomarkers Med 2013;7:575–8
35. Iura K, Kohashi K, Hotokebuchi Y, Ishii T, Maekawa A, Yamada Y, et al. Cancer-testis antigens PRAME and NY-ESO-1 correlate with tumour grade and poor prognosis in myxoid liposarcoma. J Pathol Clin Res 2015;1:144–59
36. Field MG, Decatur CL, Kurtenbach S, Gezgin G, van der Velden PA, Jager MJ, et al. PRAME as an independent biomarker for metastasis in uveal melanoma. Clin Cancer Res 2016;22:1234–42
37. Tan P, Zou C, Yong B, Han J, Zhang L, Su Q, et al. Expression and prognostic relevance of PRAME in primary osteosarcoma. Biochem Biophys Res Commun 2012;419:801–8
38. Zou C, Shen J, Tang Q, Yang Z, Yin J, Li Z, et al. Cancer-testis antigens expressed in osteosarcoma identified by gene microarray correlate with a poor patient prognosis. Cancer 2012;118:1845–55
39. Epping MT, Hart AA, Glas AM, Krijgsman O, Bernards R. PRAME expression and clinical outcome of breast cancer. Br J Cancer 2008;99: 398–403
40. Oberthuer A, Hero B, Spitz R, Berthold F, Fischer M. The tumor-associated antigen PRAME is universally expressed in high-stage neuroblastoma and associated with poor outcome. Clin Cancer Res 2004; 10:4307–13
41. Wong RWJ, Ngoc PCT, Leong WZ, Yam AWY, Zhang T, Asamitsu K, et al. Enhancer profiling identifies critical cancer genes and characterizes cell identity in adult T-cell leukemia. Blood 2017;130:2326–38
42. Steinbach D, Hermann J, Viehmann S, Zintl F, Gruhn B. Clinical implications of PRAME gene expression in childhood acute myeloid leukemia. Cancer Genet Cytogenet 2002;133:118–23.
43. Rezvani K, Yong AS, Tawab A, Jafarpour B, Eniafe R, Mielke S, et al. Ex vivo characterization of polyclonal memory CD8+ T-cell responses to PRAME-specific peptides in patients with acute lymphoblastic leukemia and acute and chronic myeloid leukemia. Blood 2009;113:2245–55
44. Gutzmer R, Rivoltini L, Levchenko E, Testori A, Utikal J, Ascierto PA, et al. Safety and immunogenicity of the PRAME cancer immunotherapeutic in metastatic melanoma: results of a phase I dose escalation study. ESMO Open 2016;1:e000068
45. Weber JS, Vogelzang NJ, Ernstoff MS, Goodman OB, Cranmer LD, Marshall JL, et al. A phase 1 study of a vaccine targeting preferentially expressed antigen in melanoma and prostate-specific membrane antigen in patients with advanced solid tumors. J Immunother 2011;34:556–67
46. Pujol JL, De Pas T, Rittmeyer A, Vallieres E, Kubisa B, Levchenko E, et al. Safety and Immunogenicity of the PRAME Cancer Immunotherapeutic in Patients with Resected Non-Small Cell Lung Cancer: A Phase I Dose Escalation Study. J Thoracic Oncol 2016;11:2208–17
47. Gonzalez-Galarza FF, Takeshita LY, Santos EJ, Kempson F, Maia MH, da Silva AL, et al. Allele frequency net 2015 update: new features for HLA epitopes, KIR and disease and HLA adverse drug reaction associations. Nucleic Acids Res 2015;43:D784–8
48. Di Stasi A, Tey SK, Dotti G, Fujita Y, Kennedy-Nasser A, Martinez C, et al. Inducible apoptosis as a safety switch for adoptive cell therapy. N Engl J Med 2011;365:1673–83
49. Zhou X, Di Stasi A, Tey SK, Krance RA, Martinez C, Leung KS, et al. Long-term outcome after haploidentical stem cell transplant and infusion of T cells expressing the inducible caspase 9 safety transgene. Blood 2014; 123:3895–905
50. Zhou X, Dotti G, Krance RA, Martinez CA, Naik S, Kamble RT, et al. Inducible caspase-9 suicide gene controls adverse effects from alloreplete T cells after haploidentical stem cell transplantation. Blood 2015;125:4103–13
51. Zhou X, Naik S, Dakhova O, Dotti G, Heslop HE, Brenner MK. Serial activation of the inducible caspase 9 safety switch after human stem cell transplantation. Mol Ther 2016;24:823–31
52. Parker BS, Rautela J, Hertzog PJ. Antitumour actions of interferons: implications for cancer therapy. Nat Rev Cancer 2016;16:131–44

Cancer Research
The Journal of Cancer Research (1916–1930) | The American Journal of Cancer (1931–1940)

AACR American Association for Cancer Research

Adoptive Immunotherapy Using PRAME-Specific T Cells in Medulloblastoma

Domenico Orlando, Evelina Miele, Biagio De Angelis, et al.

Cancer Res 2018;78:3337-3349. Published OnlineFirst April 3, 2018.